Turbulent Transfer Coefficients and Calculation of Air Temperature inside Tall Grass Canopies in Land–Atmosphere Schemes for Environmental Modeling

D. T. MIHAILOVIC*

Faculty of Agriculture, and University Center for Meteorology and Environmental Modeling, University of Novi Sad, Novi Sad, Serbia

K. ALAPATY

Carolina Environmental Program, The University of North Carolina at Chapel Hill, Chapel Hill, North Carolina

B. LALIC AND I. ARSENIC

Faculty of Agriculture, and University Center for Meteorology and Environmental Modeling, University of Novi Sad, Novi Sad, Serbia

B. RAJKOVIC

College of Physics, Belgrade University, Belgrade, Serbia

S. MALINOVIC

University Center for Meteorology and Environmental Modeling, University of Novi Sad, Novi Sad, Serbia

(Manuscript received 9 August 2003, in final form 19 April 2004)

ABSTRACT

A method for estimating profiles of turbulent transfer coefficients inside a vegetation canopy and their use in calculating the air temperature inside tall grass canopies in land surface schemes for environmental modeling is presented. The proposed method, based on *K* theory, is assessed using data measured in a maize canopy. The air temperature inside the canopy is determined diagnostically by a method based on detailed consideration of 1) calculations of turbulent fluxes, 2) the shape of the wind and turbulent transfer coefficient profiles, and 3) calculation of the aerodynamic resistances inside tall grass canopies. An expression for calculating the turbulent transfer coefficient inside sparse tall grass canopies is also suggested, including modification of the corresponding equation for the wind profile inside the canopy. The proposed calculations of *K*-theory parameters are tested using the Land–Air Parameterization Scheme (LAPS). Model outputs of air temperature inside the canopy for 8–17 July 2002 are compared with micrometeorological measurements inside a sunflower field at the Rimski Sancevi experimental site (Serbia). To demonstrate how changes in the specification of canopy density affect the simulation of air temperature inside tall grass canopies and, thus, alter the growth of PBL height, numerical experiments are performed with LAPS coupled with a one-dimensional PBL model over a sunflower field. To examine how the turbulent transfer coefficient inside tall grass canopies over a large domain represents the influence of the underlying surface on the air layer above, sensitivity tests are performed using a coupled system consisting of the NCEP Nonhydrostatic Mesoscale Model and LAPS.

1. Introduction

Many complex environmental features at small, medium, or large scales involve processes that occur both within and between environmental media (e.g., air, surface water, groundwater, soil, biota). Considerable recent research work addresses various aspects of modeling these processes using new methodologies/approaches, numerical methods, and software techniques (e.g., Rodhe et al. 2000; Walko et al. 2000; Brandmeyer and Karimi 2001; Janjić et al. 2001; Lalic et al. 2003; Mihailovic et al. 2001, 2002; and references therein). In environmental models, calculating turbulent fluxes inside and above a vegetation canopy requires the specification of air temperature, water vapor pressure, and turbulent transfer coefficients inside the canopy (Sellers et al. 1986; Mihailovic 1996; Xue et al. 1991). The calculation of these quantities inside a tall grass canopy has been considered by many authors (e.g., Sellers and

* Current affiliation: Norwegian Meteorological Institute, Oslo, Norway.

Corresponding author address: Dragutin T. Mihailovic, Norwegian Meteorological Institute, Postboks 43, Blindern, 0313 Oslo, Norway.
E-mail: dragutin.t.mihailovic@met.no

Dorman 1987; Laval 1988; Sellers et al. 1989; Munley 1991; Mihailovic et al. 1993; Zoumakis 1993; Henderson-Sellers 1996; Brutsaert and Sugita 1996; Raupach et al. 1996). Their work has remarkably improved the parameterization of turbulent fluxes inside tall grass canopies in land surface schemes, making them more relevant, for example, in assessing how various crops may affect regional climate (Gedney et al. 2000; Pielke 2002b). However, there is not yet a complete approach for modeling the turbulent fluxes inside tall grass canopies, particularly in the case of sparse tall grass canopies [i.e., those in which the plant spacing is on the order of the canopy height or larger (Wyngaard 1988)]. Such an approach is needed because tall grass canopies, through key variables like friction velocity and internal air temperature, can significantly affect heat and moisture exchange in the lower atmosphere.

The objective of this paper is to examine the impact of the turbulent moisture/heat transfer coefficient (referred to hereinafter as the turbulent transfer coefficient) on the calculation of aerodynamic resistances and air temperature inside tall grass canopies in land–atmosphere schemes for environmental modeling. Section 2 summarizes the aerodynamic resistances for calculating the air temperature inside the canopy (section 2a) and a derivation of the wind and turbulent transfer coefficient profiles inside tall grass canopies (section 2b) and sparse tall grass canopies (section 2c). Section 3 is devoted to numerical tests. Section 3a includes 1) numerical simulation of the air temperature inside a sunflower field for a 10-day period, performed using a land surface scheme, and its comparison with observations; and 2) simulation of the air temperature inside a sunflower field that has lower plant density and the corresponding growth of the PBL height, performed by running the coupled Land–Air Parameterization Scheme (LAPS) and a one-dimensional (1D) PBL model. Section 3b discusses numerical tests using a 3D mesoscale model. Section 4 summarizes all of the results.

2. The turbulent transfer coefficient and calculating air temperature inside tall grass canopies

a. *Deriving aerodynamic resistances for calculating air temperature inside the canopy*

The canopy air space temperature T_a in land surface schemes can be determined diagnostically from the energy balance equation. This procedure comes from the equality of the sensible heat flux from the canopy to some reference level in the atmosphere and the sum of the sensible heat fluxes from the ground and from the leaves to the canopy air volume (Sellers et al. 1986; Mihailovic 1996), that is,

$$T_a = \frac{\dfrac{2T_f}{r_b} + \dfrac{T_g}{r_d} + \dfrac{T_r}{r_a}}{\dfrac{2}{r_b} + \dfrac{1}{r_d} + \dfrac{1}{r_a}}, \tag{1}$$

where T_f is the foliage temperature, T_g is the ground surface temperature, T_r is the temperature at reference level, r_b is the bulk boundary layer aerodynamic resistance, r_d is the aerodynamic resistance to water vapor and heat flow from the soil surface to the air space inside the canopy, and r_a is the aerodynamic resistance representing the transfer of heat and moisture from the canopy to the reference level z_r (see appendix A).

The aerodynamic resistance r_a between z_r and the water vapor and sensible heat source height h_a (Sellers et al. 1986) can be defined as

$$r_a = \int_{h_a}^{H} \frac{1}{K_s}\, dz + \int_{H}^{z_r} \frac{1}{K_s}\, dz, \tag{2}$$

where H is the canopy height and K_s is the turbulent transfer coefficient (momentum/moisture/heat) inside and above the canopy in the intervals (h_a, H) and (H, z_r), respectively. The aerodynamic resistance in canopy air space r_d can be written in the form

$$r_d = \int_{z_g}^{h} \frac{1}{K_s}\, dz + \int_{h}^{h_a} \frac{1}{K_s}\, dz, \tag{3}$$

where z_g is the effective ground roughness length and h is the canopy bottom height (the height of the base of the canopy). The area-averaged bulk boundary layer resistance $\overline{r_b}$ has the form (Sellers et al. 1986)

$$\frac{1}{\overline{r_b}} = \int_{h_a}^{H} \frac{\overline{L_d}\sqrt{u(z)}}{C_s P_s}\, dz, \tag{4}$$

where $\overline{L_d}$ is the area-averaged stem and leaf area density (also called canopy density), which is related to leaf area index (LAI) as LAI $= \overline{L_d}(H - h)$, $u(z)$ is the wind speed, C_s is the transfer coefficient (Sellers et al. 1986), and P_s is the leaf shelter factor. Equations (1)–(4) can be modified to take into account the effects of nonneutrality. According to Sellers et al. (1986), the position of the canopy source height h_a can be estimated by obtaining the center of gravity of the $1/\overline{r_b}$ integral. Thus,

$$\int_{h}^{h_a} \frac{\overline{L_d}}{r_b}\, dz = \int_{h_a}^{H} \frac{\overline{L_d}}{r_b}\, dz = \frac{1}{2}\int_{h}^{H} \frac{\overline{L_d}}{r_b}\, dz = \frac{1}{2\overline{r_b}}. \tag{5}$$

We may obtain h_a by successive estimation (Sellers et al. 1986; Mihailovic and Rajkovic 1993) until the foregoing equality is reached.

In this paper, we restrict our attention to the influence of the turbulent transfer coefficient K_s on calculating the resistances r_d and r_a, as well as the air temperature inside the tall grass canopy T_a in land–atmosphere schemes for various spatial scales of environmental modeling. Our analysis first addresses dense tall grass canopies and then moves to sparse canopies.

b. Calculating the wind profile inside tall grass canopies

In this section, we derive an expression for K_s within tall grass canopies as a function of their morphological and aerodynamic parameters. For this purpose we consider the canopy to be a block of constant-density porous material sandwiched between two heights, H and h (Sellers et al. 1986; Mihailovic and Kallos 1997). The differential equation describing the wind profile within such a ''sandwiched'' canopy architecture can be written in the form (see appendix B)

$$\frac{d}{dz}\left(K_s\frac{du}{dz}\right) = \frac{C_d\overline{L_d}(H - h)}{H}u^2, \tag{6}$$

where the coefficient of proportionality C_d is the leaf drag coefficient. To solve this equation, we have to know how K_s depends on parameters that represent the canopy's aerodynamic and morphological features. The K theory is a commonly used method in modeling the turbulence within a plant canopy. Although its use may be physically unrealistic for this application, it yields reasonable results, and so we shall use this method until suitable second-order closure models are developed and then applied to the problem. Several papers have been published recently that focus on the closure problem, particularly within forest canopies (Massman and Weil 1999; Katul and Chang 1999; Pinard and Wilson 2001). However, because the traditional K-theory approach can be applied successfully within tall grass canopies (Sellers and Dorman 1987, and references therein), we shall stay with it. The question about the behavior of K_s within forest canopies is beyond the scope of this paper.

A number of assumptions are offered about the variation of K_s within tall grass canopies (Legg and Long 1975; Denmead 1976). Among those, we chose the approach in which K_s is proportional to wind speed u, that is,

$$K_s = \sigma u, \tag{7}$$

where the scaling length σ is an arbitrary, unknown constant. Combining Eqs. (6) and (7) produces an equation for the wind speed inside the canopy:

$$\frac{d^2u^2}{dz^2} = \frac{2C_d\overline{L_d}(H - h)}{\sigma H}u^2. \tag{8}$$

A particular solution of this equation can be found in a form that approximates the wind profile within the tall grass canopy fairly well (Brunet et al. 1994):

$$u(z) = u(H)\exp\left[-\frac{1}{2}\beta\left(1 - \frac{z}{H}\right)\right], \tag{9}$$

where $u(H)$ is the wind speed at the canopy height and β is the extinction parameter, defined as

$$\beta^2 = \frac{2C_d\overline{L_d}(H - h)H}{\sigma}, \tag{10}$$

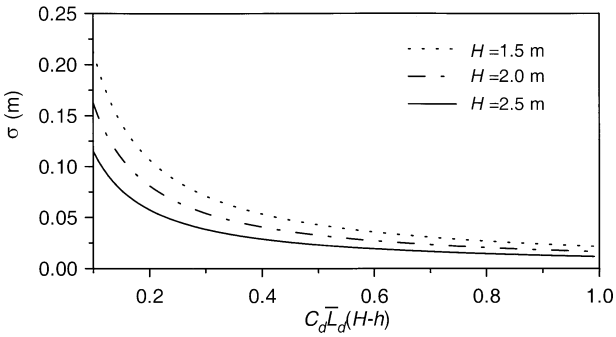

FIG. 1. Calculated values of the scaling length σ as a function of the leaf drag coefficient C_d, area-averaged canopy density $\overline{L_d}$, canopy height H, and canopy bottom height h, for three tall grass canopy heights.

where σ still remains an unknown constant. Its value can be determined as a function of the morphological and aerodynamic characteristics of the underlying tall grass canopy in the following manner. We shall use the lower boundary condition at the canopy bottom $z = h$ in terms of the shear stress τ just above and below the indicated level. Therefore,

$$\tau|_h = \rho C_{\rm dg}u^2|_h, \tag{11}$$

where ρ is air density and $C_{\rm dg}$ is the leaf drag coefficient estimated from the size of the roughness elements of the ground (Sellers et al. 1986); that is,

$$C_{\rm dg} = \frac{k^2}{\left(\ln\dfrac{h}{z_g}\right)^2}, \tag{12}$$

where k is the von Kármán constant, taken to be 0.41, and

$$\tau|_h = \rho K_s\left.\frac{du}{dz}\right|_h. \tag{13}$$

Combining Eqs. (7), (9), (11), and (13), after some simple algebra, we get an equation for the parameter σ of the form

$$2C_{\rm dg}H = \beta\sigma. \tag{14}$$

Last, substituting β from Eq. (10) in Eq. (14) and solving for the scaling length σ, we reach

$$\sigma = \frac{2C_{\rm dg}^2H}{C_d\overline{L_d}(H - h)}, \tag{15}$$

which expresses σ through the morphological and aerodynamic parameters describing the stand canopy in the sandwich approach. Figure 1 depicts calculated values of σ as a function of the leaf drag coefficient, canopy density, canopy height, and canopy bottom height for three tall grass canopy heights. In these calculations we used Eqs. (12) and (15). It can be seen that lower values of tall grass canopy height and density $[C_d\overline{L}_d(H - h)]$ cause rapid growth of the scaling length. Such a plant

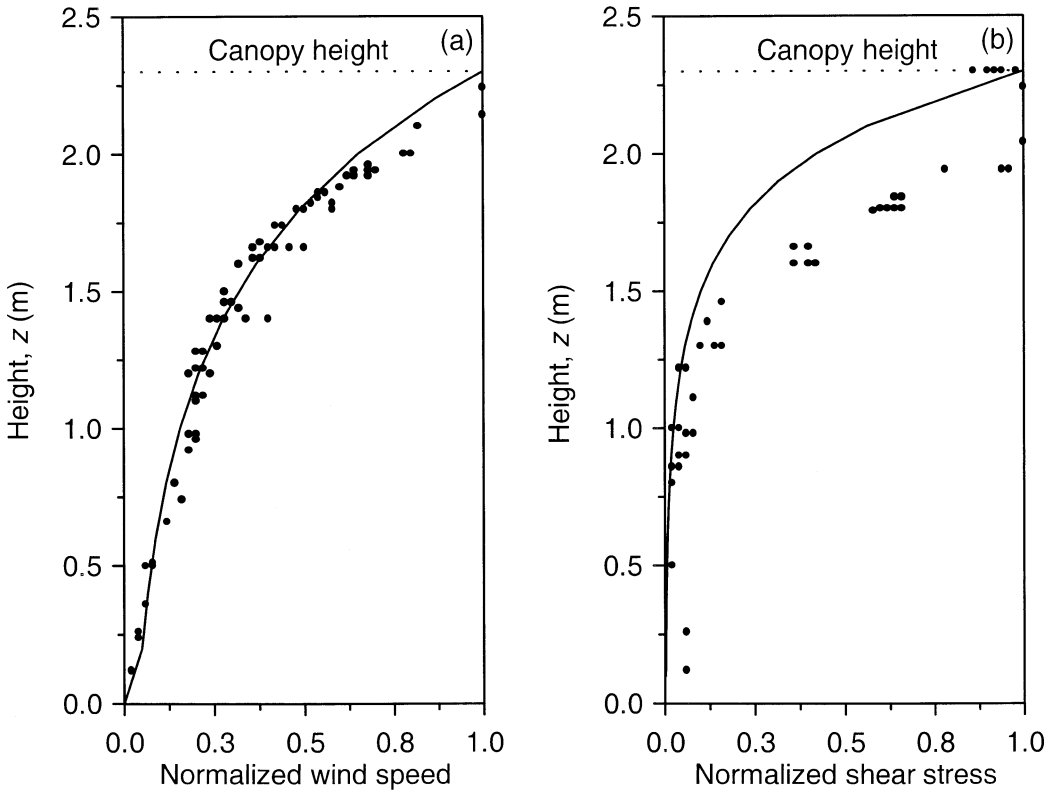

FIG. 2. Profiles of (a) wind speed and (b) shear stress inside a maize crop. The black circles are observations from Wilson et al. (1982), and the solid lines are plotted using calculated values. The wind speed u and shear stress τ are normalized by their values $u(H)$ and $\tau(H)$ at the canopy top height.

canopy architecture includes more air space, and so physically the turbulent transport of momentum, heat, and water vapor more closely resembles the energy and momentum exchange above bare soil. In contrast, for values of $C_d\overline{L}_d(H - h)$ that are typical of tall grass canopy (0.5–0.7) according to Sellers and Dorman (1987), σ has a lower value. This result means that the turbulent transfer coefficient K_s within a dense tall grass canopy, where eddies are small and dissipate quickly, tends to have lower values. To illustrate how well values calculated from the above expressions agree with observations, we compared the calculated profiles of wind speed and shear stress with values observed by Wilson et al. (1982) inside a maize crop. They gathered observations of crop height H (2.3 m) and LAI (2.9) and estimated the effective leaf drag coefficient C_d to be 0.17. These values were used in the above calculations, assuming values of $h = 0.115$ m for the canopy bottom height and $z_g = 0.0256$ m for the effective ground roughness length. We obtained $C_d\overline{L}_d(H - h) = 0.493$, $\beta = 6.619$, and $\sigma = 0.0518$ m. Figure 2a shows a comparison between calculated and observed wind speed values inside the maize canopy. The shape of the calculated wind profile curve follows the observations well. Between the canopy height and canopy bottom height, the wind profile attenuates exponentially according to Eq. (9), while beneath the canopy bottom height it follows a classical logarithmic profile of the form

$$u(z) = \frac{u(H)\exp\left[-\frac{1}{2}\beta\left(1 - \frac{h}{H}\right)\right]}{\ln\frac{h}{z_g}}\ln\frac{z}{z_g}. \quad (16)$$

The shear-stress comparison is shown in Fig. 2b. Just below the canopy top, the calculated curve does not follow the shape of the observations; a very sharp attenuation of the calculated shear stress is evident in the layer between 1.2 and 2.3 m. Within the upper part of the canopy, the observed turbulent exchange of momentum is apparently more intense than the values obtained using K theory. In the canopy layer below $z = H$, observed momentum exchange (and, therefore, the turbulent transfer coefficient) becomes very erratic, often exhibiting singularities. This behavior is associated with observations of countergradient fluxes within canopies (Raupach et al. 1996), indicating that the turbulent transfer processes are essentially nonlocal and cannot be described by a local gradient–diffusion relationship.

However, as mentioned earlier, we do not address this topic here because it is beyond the scope of this paper.

Last, because we know $u(z)$, the variation of wind speed with height inside the canopy, we can derive an expression for the canopy source height h_a. Assuming that the canopy density is constant with height and by combining Eqs. (4) and (5), we reach equality:

$$2\int_{h}^{h_a}\sqrt{u(z)}\,dz = \int_{h_a}^{H}\sqrt{u(z)}\,dz. \tag{17}$$

If we solve these integrals, keeping in mind that the functional form of $u(z)$ is given by Eq. (9), we get

$$h_a = H\left\{1 + \frac{4}{\beta}\ln\frac{1 + 2\exp\left[-\frac{1}{4}\beta\left(1 - \frac{h}{H}\right)\right]}{3}\right\}. \tag{18}$$

c. Calculating the turbulent transfer coefficient inside sparse tall grass canopies

In a sparse tall grass canopy (one in which the plant spacing is on the order of the canopy height or larger), K_s is strongly affected by processes in the environmental space, including the plants and the space above the bare soil fraction. Therefore, K_s inside a sparse canopy, denoted K_s^s, can be represented by some combination of turbulent transfer coefficients in that space. If, as a working hypothesis, we assume a linear combination weighted by the fractional vegetation cover σ_f (a measure of how sparse the tall grass is), then we can define K_s^s as

$$K_s^s = \sigma_f\sigma u + ku_*(1 - \sigma_f)z, \tag{19}$$

where u_* is the friction velocity above the bare soil fraction and z is the vertical coordinate. In the case of dense vegetation ($\sigma_f = 1$), Eq. (19) reduces to Eq. (7). Otherwise, when $\sigma_f = 0$, Eq. (19) represents the turbulent transfer coefficient over bare soil. We can use Eq. (19) in calculating the wind speed inside a sparse tall grass canopy. For that purpose we have to modify Eq. (6) slightly to take into account σ_f:

$$\frac{d}{dz}\left(K_s^s\frac{du}{dz}\right) = \sigma_f\frac{C_d\overline{L_d}(H - h)}{H}u^2. \tag{20}$$

Replacing the expression for K_s^s given by Eq. (19) in Eq. (20) produces

$$\frac{d}{dz}\left\{[\sigma_f\sigma u + ku_*(1 - \sigma_f)z]\frac{du}{dz}\right\} = \sigma_f\frac{C_d\overline{L_d}(H - h)}{H}u^2. \tag{21}$$

After differentiation and grouping, the terms we reach are

$$a(u, z)\frac{d^2u}{dz^2} + b(z)\frac{du}{dz} + c\left(\frac{du}{dz}\right)^2 = gu^2, \tag{22}$$

where

$$a(u, z) = \sigma_f\sigma u + ku_*(1 - \sigma_f)z, \qquad c = \sigma_f\sigma,$$
$$b(z) = ku_*(1 - \sigma_f)z, \quad \text{and}$$
$$g = \sigma_f\frac{C_d\overline{L_d}(H - h)}{H}.$$

To get the wind profile inside the sparse canopy, we solved Eq. (22) numerically, using the fourth-order Runge–Kutte method (Ayers 1952).

3. Numerical tests

a. Results of calculating air temperature inside a sunflower field for a long-term integration

To examine how successfully the foregoing proposed calculations of *K*-theory parameters support simulating the air temperature within a tall grass canopy, a test was performed using the LAPS land surface scheme described in Mihailovic et al. (2000) and Pielke (2002a). LAPS outputs of canopy air space temperature for 10 days (8–17 July 2002) were compared with single-point micrometeorological measurements over a sunflower field at the Rimski Sancevi experimental site in Serbia. In the numerical tests we used a dataset from a measurement program that examined the exchange processes of heat, mass, and momentum just above and inside a sunflower canopy during its growing season. The experimental site (270 m × 68 m) is located in the northern part of Serbia (45.3°N, 19.8°E) on a chernozem soil of the loess terrace of southern Backa with the following physical and water properties: Clapp–Hornberger constant B of 6.50, ground emissivity of 0.97, heat capacity of the soil fraction of 780 J kg^{-1} °C^{-1}, saturated hydraulic conductivity of 32×10^{-6} m s^{-1}, soil moisture potential at saturation of -0.036 m, soil density of 1290 kg m^{-3}, ratio of saturated thermal conductivity to that of loam of 1.0, volumetric soil moisture content at saturation of 0.52 m^3 m^{-3}, volumetric soil moisture content at field capacity of 0.36 m^3 m^{-3}, wilting-point volumetric soil moisture content of 0.17 m^3 m^{-3}; and effective ground roughness length of 0.01 m. The experimental site was surrounded by other agricultural fields also sown with sunflowers. The sunflower rows were oriented north to south, with row spacing of 0.70 m. This dataset was chosen because it was considered to be typical and representative of a fully developed sunflower crop.

For the 8–17 July period, the mean estimated LAI was 3.0 m^2 m^{-2}, the crop height H was around 1.99 m, and the canopy bottom height h was 0.100 m. The scaling length σ and the extinction factor β were calculated using Eqs. (15) and (10), while the zero plane displacement d and roughness length z_0 were calculated according to Mihailovic and Kallos (1997), that is, $d = H - (2\sigma H/\beta)^{1/2}/k$ and $z_0 = (H - d)\exp\{-2H/[\beta(H - d)]\}^{1/2}$. In these calculations, the area-averaged canopy density $\overline{L_d}$ had a value of 1.59 m^2 m^{-3}, and a value of

0.2 was used for the leaf drag coefficient C_d. We calculated the following values: $\sigma = 0.055$ m, $\beta = 6.578$, $d = 1.54$ m, and $z_0 = 0.115$ m. Because the minimum stomatal resistance was not measured, we assumed it to be 40 s m^{-1}. The fractional vegetation cover was 0.90. Other parameters used in the simulation can be found in Mihailovic et al. (2000).

Temperatures were measured using platinum resistance thermometers (Pt-100) set at 0.95 and 2.1 m above the ground. The wind speed at the reference level of $z_r = 2.1$ m was measured using a Vector Instruments, Ltd., anemometer. A Kipp and Zonen, Inc., CM5 solarimeter was used to measure incoming solar radiation, and relative humidity was recorded using a Greisinger Electronic GmbH sensor set at 2.1 m. Precipitation was measured by an electronic rain gauge manufactured at the Institute of Physics in Belgrade. Soil temperature was measured at 0.05-, 0.1-, and 0.2-m depths. In all datasets, the atmospheric boundary conditions at $z_r = 2.1$ m were derived from measurements of global radiation, precipitation, relative humidity, and wind for 24 h from 0000 LST at 30-min intervals. The longwave atmospheric counterradiation was calculated with an empirical formula described in Mihailovic et al. (1995), including a correction for the amount of cloudiness. Cloudiness data were taken at 30-min intervals from the nearest standard meteorological station, Rimski Sancevi, which is 500 m away from the experimental site. These values were interpolated to the beginning of each time step ($\Delta t = 120$ s). Soil layer thickness were defined as $D_1 = 0$–0.1 m, $D_2 = 0.1$–0.5 m, and $D_3 = 0.5$–1 m. The initial conditions for the volumetric soil moisture contents corresponding to these layers were $w_1 = 0.1552$ m^3 m^{-3}, $w_2 = 0.1484$ m^3 m^{-3}, and $w_3 = 0.1348$ m^3 m^{-3}. At the initial time the ground temperature T_g was 292.68 K. The initial condition for atmospheric pressure was 100.53 kPa.

The temperature inside the sunflower air space T_a was determined diagnostically using Eq. (1). In that formula, the three aerodynamic resistances r_a, r_b, and r_d are calculated as follows:

$$r_a = \frac{1}{u_*}\left\langle \frac{2kH}{\sigma\beta \ln\dfrac{H-d}{z_0}}\left\{\exp\left[\frac{1}{2}\beta\left(1-\frac{h_a}{H}\right)\right]-1\right\} + \frac{1}{k}\ln\frac{z_r-d}{H-d}\right\rangle, \tag{23}$$

$$r_b = \frac{1}{\sqrt{u_*}}\frac{\beta C_s P_s \sqrt{k}}{4H\overline{L}_d\sqrt{\ln\dfrac{H-d}{z_o}}\left\{1-\exp\left[-\frac{1}{4}\beta\left(1-\frac{h_a}{H}\right)\right]\right\}}, \quad \text{and} \tag{24}$$

$$r_d = \frac{1}{u_*}\left\langle \frac{2kH}{\sigma\beta \ln\dfrac{H-d}{z_0}}\left\{\exp\left[\frac{1}{2}\beta\left(1-\frac{h}{H}\right)\right]-\exp\left[\frac{1}{2}\beta\left(1-\frac{h_a}{H}\right)\right]-1\right\} + \frac{\exp\left[\frac{1}{2}\beta\left(1-\frac{h}{H}\right)\right]}{k\ln\dfrac{H-d}{z_o}}\ln^2\frac{h}{z_g}\right\rangle. \tag{25}$$

The values for the leaf shelter factor P_s and transfer coefficient C_s used in the simulation are listed in Mihailovic and Kallos (1997). The effect of atmospheric nonneutrality in Eqs. (23)–(25) (i.e., their dependence on T_a and T_r) is included in u_* and accordingly in other calculations. Canopy source height h_a was calculated using Eq. (18) and the above parameter values, resulting in a value of 1.1 m. The validity of the LAPS-simulated canopy air space temperature was tested against the observations recorded by the platinum resistance thermometer located at 0.95 m at 30-min intervals during 8–17 July 2002. Figure 3 shows the calculated and observed diurnal variations of air temperature inside the sunflower canopy at the experimental site. After midnight, the simulated values are lower than the observations, and in the early afternoon the simulated values are higher than the observed ones. This situation occurs

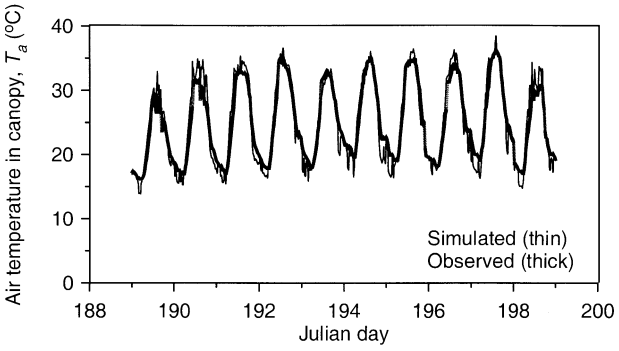

FIG. 3. Ten-day variation (8–17 Jul 2002) of the air temperature simulated by LAPS and observed inside a sunflower canopy at the Rimski Sancevi site.

because at night LAPS simulates less heat transfer from the ground into the canopy air space than the observations indicate. In contrast, during the afternoon the scheme calculates a lower amount of evapotranspiration, which for some days results in a higher leaf temperature and, as a consequence, a higher air temperature inside the sunflower canopy [Eq. (1)]. It is apparent that the calculation of air temperature inside a tall grass canopy strongly depends on the resistances given by Eqs. (23)–(25), that is, on the resistances' sensitivity to morphological and aerodynamic parameters, which can be sources of uncertainty in their calculation. The sensitivity of the aerodynamic parameters and resistances and turbulent transfer fluxes in the Simple Biosphere model (SiB) surface scheme (Sellers et al. 1986; Xue et al. 1991) to uncertainties in the input parameters has already been addressed in Sellers et al. (1986) and Sellers and Dorman (1987) and later in Mihailovic and Kallos (1997) for LAPS. However, there is still no information available in the literature on the sensitivity of turbulent transfer calculations to the canopy bottom height h. Following the approach elaborated in this paper and other similar approaches related to the sandwich treatment of the canopy (e.g., Sellers and Dorman 1987; Xue et al. 1991), it can be seen that the parameters having a key dependence on h are C_{dg} [Eq. (12)] and σ [Eq. (15)]. However, this certainly does not mean that other parameterization quantities, including the canopy bottom height, either explicitly or implicitly, are less sensitive than C_{dg} and σ. We will show a somewhat surprising degree of sensitivity in the estimation of h when the sandwich approach is used and how this sensitivity affects the surface scheme's ability to realistically simulate turbulent transfer inside and above the tall grass canopy. This will be done in two steps. First, we establish a procedure for estimating h for tall grass. Second, on the basis of this procedure, we discuss the possible uncertainties resulting from the parameterizations of some of the aerodynamic parameters.

To our knowledge, the literature contains no information on how to estimate canopy bottom height reliably. The only information available is the h values of 1–2.5 m reported for tall grass canopies by Dubov et al. (1978), Goudriaan (1977), Sellers and Dorman (1987), Xue et al. (1991), Mihailovic and Kallos (1997), and Mihailovic et al. (2000). Using these data, we found a functional dependence of h on the canopy height H, using a fifth-degree polynomial-fitting procedure (Fig. 4). This dependence can be helpful in land surface schemes that use the sandwich approach to describe the vegetation layer. We checked the representativeness of this curve indirectly by calculating the zero-plane displacement d and roughness length z_0 for tall grass canopies of known morphological characteristics, using maize data from Wilson et al. (1982) and van Pul (1992). The derived z_0/H and d/H values of 0.08 and 0.71 for the Wilson et al. case and 0.051 and 0.76 for the van Pul case are within the range of values reported by Uchijima (1976): 0.05–0.15 for z_0/H and 0.53–0.8 for d/H.

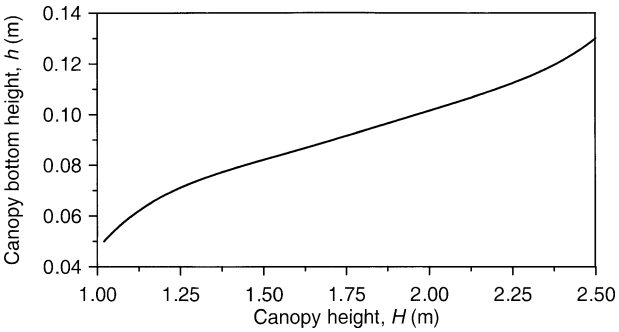

FIG. 4. Calculated values of the canopy bottom height h as a function of the canopy height H for tall grass vegetation. The fitting curve is drawn using data from Dubov et al. (1978), Sellers and Dorman (1987), Mihailovic and Kallos (1997), and Mihailovic et al. (2000).

To quantify the sensitivity of the air temperature inside a tall grass canopy to canopy bottom height, we performed sensitivity tests with $h = 0.05H$ as a reference state for the sunflower canopy, using the model settings described earlier. Further, the value of h was allowed to vary from −30% to +30% of the reference value. We computed the root-mean-square error (rmse) and mean absolute value (MAE), defined as

$$\text{rmse} = \left[\frac{1}{N}\sum_{i=1}^{N}(\Gamma_i - \hat{\Gamma}_i)^2\right]^{1/2} \quad \text{and} \tag{26}$$

$$\text{MAE} = \frac{1}{N}\sum_{i=1}^{N}|\Gamma_i - \hat{\Gamma}|, \tag{27}$$

where Γ is the variable of interest (canopy air space temperature, in this study) and N is the total number of hourly data. A caret indicates the reference state, whereas the absence of a caret indicates a simulated value. Table 1 shows the errors in the air temperature inside the sunflower canopy, as well as its calculated aerodynamic characteristics, resulting from the changes in h. The −30% to +30% changes in h introduced the following errors in canopy air space temperature: 1.501°–1.444°C for rmse and 1.238°–1.155°C for MAE. Let us explain these results. As h increases, the values of d and h_a also increase, because the height of momentum absorption rises with increasing vegetation density β; denser, less penetrable tall grass canopy (lower values of σ and C_d) presents a less porous, ''smoother'' surface to the atmospheric airflow. This same process makes z_0 decrease with increasing canopy density. In this case, the ground surface temperature and foliage temperature become lower, resulting in a lower temperature inside the sunflower canopy [Eq. (1)].

To demonstrate how changing the specification of canopy density affects the simulation of air temperature inside the tall grass canopy and, thus, the evolution of the PBL height, we performed experiments by running LAPS coupled with a 1D PBL model over a sunflower

TABLE 1. Statistical analysis of the sensitivity of canopy air space temperature T_a and associated aerodynamic characteristics to the canopy bottom height.

h (m)	C_d	β	σ (m)	D (m)	z_0 (m)	h_a (m)	Rmse for T_a (°C)	MAE for T_a (°C)
0.035	0.1680	3.576	0.1870	0.878	0.409	0.734	1.501	1.238
0.040	0.1310	4.593	0.1130	1.223	0.246	0.811	1.065	0.837
0.045	0.1070	5.597	0.0762	1.422	0.162	0.920	0.502	0.465
0.055	0.0744	7.534	0.0420	1.626	0.085	1.032	0.823	0.637
0.060	0.0709	6.463	0.0344	1.685	0.066	1.132	1.158	0.934
0.065	0.0641	9.366	0.0272	1.728	0.052	1.222	1.444	1.155

canopy, similar to the method of van den Hurk (1996). The 1D model, developed particularly for studying the above effects, follows the work of Zhang and Anthes (1982), Estoque (1968), Blackadar (1976, 1978), and Alapaty et al. (1997a). The model's governing equations are the same as those in Zhang and Anthes (1982). It contains two modules that represent two different regimes of turbulent mixing: a nocturnal module and a free-convection module. All prognostic variables are defined at the midlevel of the vertical grid; diagnostic quantities such as the Richardson number; the eddy exchange coefficients; and the fluxes of heat, moisture, and momentum are defined at layer interfaces. We assume that there are no energy fluxes across the top of the mixed layer. An implicit diffusion scheme (Richtmyer and Morton 1967) is utilized to calculate the turbulent terms, with the equations for eddy coefficients suggested by Zhang and Anthes (1982). In the computational procedure, the sign of the temperature gradient in the lowest model level and the stability parameter are checked at every time step to determine which module is applicable. Then, the friction velocity and surface temperature are calculated using LAPS, and prognostic variables for the lowest model level are computed.

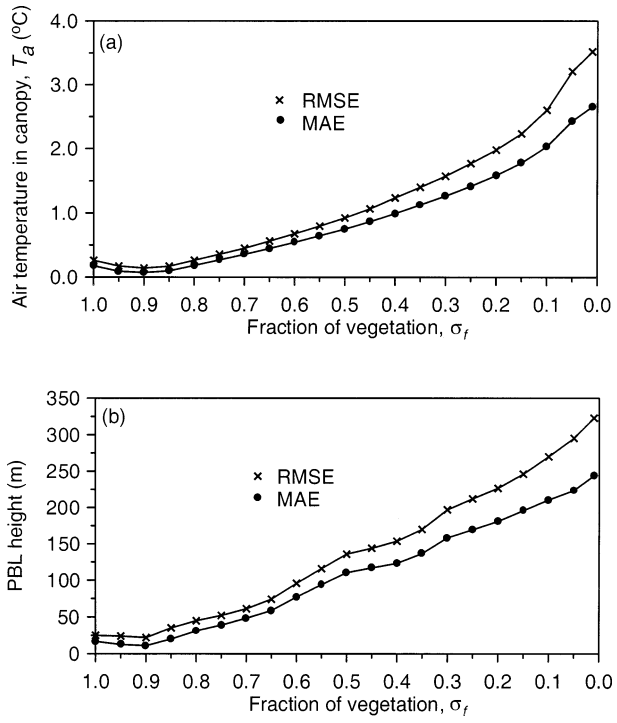

FIG. 5. The rmse [Eq. (26)] and MAE [Eq. (27)] between the calculated and reference values of (a) air temperature inside the canopy and (b) PBL height for different fractions of tall grass vegetation in the grid cell. The reference state is a grid cell with $\sigma_f = 0.90$.

In the experiments, we assumed that the entire grid cell was covered by sunflowers. Calculations were performed for surface temperature and the corresponding PBL height as a function of fractional cover σ_f, whose impact as a whole was examined by changing its value from 1 to 0.01. The term ''surface temperature'' refers to the ground temperature of a thin surface slab of soil; for the canopy it represents the canopy air space temperature T_a. Differences in the numerically simulated values of T_a and in the PBL height caused by changes in σ_f in the grid cell were quantified using the rmse and MAE between the calculated and reference values; these are plotted in Fig. 5. It can be seen that for higher values of σ_f the rmse and MAE are lower. As expected, when vegetation is highly dominant over bare soil in a grid cell, the underlying surface does not significantly contribute to the sensible heat fluxes directed from the grid cell into the atmosphere. This results in a lower surface temperature and slower growth of the PBL height error. On the other hand, increasing the bare soil fraction leads to more rapid growth of the PBL height error. This occurs because evapotranspirational cooling of the grid cell is reduced, so that the sensible heat flux from the bare soil plays the dominant role in the land–atmosphere energy exchange, resulting in higher error when calculating PBL height (Alapaty et al. 1997b).

b. Numerical experiments using 3D simulation

To examine how K_s inside a tall grass canopy over a large domain represents the influence of the underlying surface on the air layer above, we designed a numerical experiment using a 3D simulation. We analyzed the model outputs of the heat fluxes, turbulent transfer coefficients, air temperature, and PBL height to focus on the application to environmental modeling, particularly for assessing how various crops affect regional climate. In this case study, we performed a numerical simulation using the National Centers for Environmental Prediction (NCEP) Nonhydrostatic Mesoscale Model (NMM; Jan-

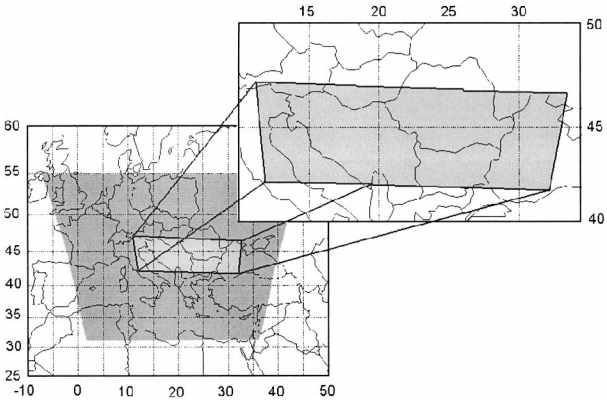

FIG. 6. Model domain. The lighter shaded area is the control domain used for sensitivity tests; the darker shaded area is the domain of integration.

jić 1994; Janjić et al. 2001), with LAPS implemented in it (Mihailovic 2003). The σ terrain-following coordinate was used with 38 levels in the vertical. For the initial and boundary meteorological conditions, the NCEP objective global analysis gridded data with a 1° horizontal increment, for 23 pressure levels (up to 50 hPa), were used. The lateral boundaries of the model domain from the NCEP data were available every 6 h. The starting time of the simulation was 0000 UTC 5 June 2002, and the simulation period was 24 h. The model has a horizontal increment of 0.222° × 0.205° and a time step of 100 s. The domain (Fig. 6) was centered in 45.0°N, 19.0°E with (101, 99) cells distributed longitudinally and latitudinally. In the preparation phase, surface parameters, either observed or predefined (topography, sea surface temperature, soil and vegetation types, soil temperatures and wetness, and slopes and azimuths of the sloping surfaces), were interpolated to the model grid. The topographic dataset used in the one provided by the U.S. Navy with 10 arc min × 10 arc min resolution. The vegetation dataset is available from the U.S. Geological Survey (USGS) with a 30 arc s × 30 arc s resolution, following the classification by Dickinson et al. (1986). For soil textural classes, the United Nations Environment Program Food and Agriculture Organization dataset was used, after converting from soil type to soil textural Zobler classes (Staub and Rosenzweig 1987). Albedo and surface roughness variations were computed in the preprocessing stage according to vegetation type. Figure 6 depicts the domain of integration and the domain used for the sensitivity tests; the latter is referred to as the control domain, chosen because agricultural land predominates in this area. The control domain has 651 grid cells. The cover types it contained were water (22.7%), crops (i.e., short grass canopies) (39.9%), tall grass (4.3%), short grass patches (3.2%), evergreen needle leaf (2.6%), deciduous broadleaf (4.3%), and mixed woodland (23.0%); the soil textural classes were water (22.7%), loamy sand (4.5%), sandy loam (11.5%), silt clay loam (36.6%), clay loam

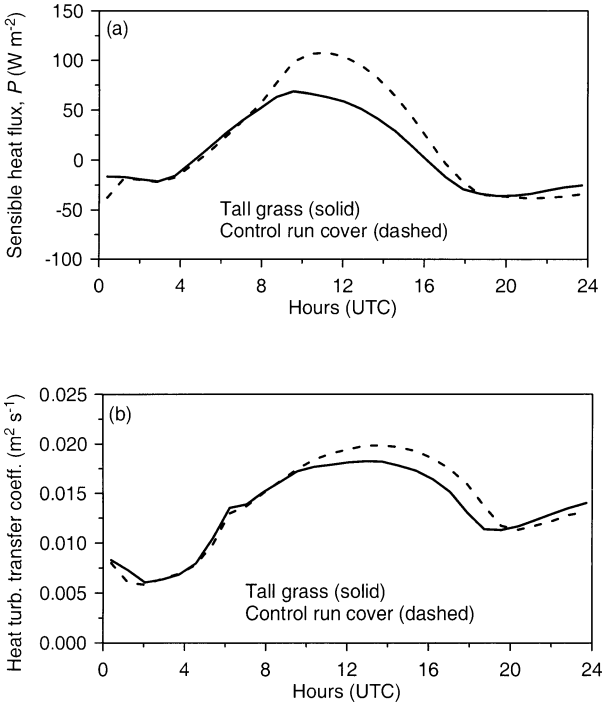

FIG. 7. Temporal variation of the area-averaged (a) surface sensible heat flux and (b) heat turbulent transfer coefficient between the surface and the lowest-model-level temperature, for the control-run cover and tall grass canopy. The temporal values are obtained by averaging over all grid cells in the control domain.

(19.7%), sandy clay (2.5%), and silty clay (2.5%). The control simulation (referred to as the control run) was performed with this distribution of cover types. For the sensitivity run, it was instead assumed that tall grass completely covered the control domain. Figure 7a depicts the temporal variation of the area-averaged surface sensible heat flux for the control run cover and tall grass canopy. The instantaneous value of the surface sensible heat flux P was calculated using

$$P = \rho c_p \frac{T_a - T_r}{r_a}, \tag{28}$$

where ρ is the density of air and c_p is the specific heat of air at constant pressure. The reliability of this expression depends on the canopy air space temperature (T_a) explicitly and also implicitly through r_a, the aerodynamic resistance representing the transfer of heat and moisture from the canopy to the reference level. The importance of aerodynamic resistances in calculating the fluxes for a wide range of vegetation was comprehensively considered from both the atmospheric modeling (Sellers and Dorman 1987) and environmental modeling (Walko et al. 2000) points of view. For example, Sellers and Dorman (1987) explored the maximum uncertainties, expressed as percentages, in the canopy aerodynamic resistances r_a, r_b, and r_d due to uncertainties in 1) the canopy drag coefficient C_D, defined as $C_D = (C_d/P_s)\bar{L}_d(H - h)$, where C_d is the leaf drag coefficient, and

2) the shape of the wind profile inside and above the canopy. They found that the uncertainty in the estimates of $1/r_a$ (the dominant turbulent transfer term) and $1/r_b$ ranged from 25% to 88%. Because the parameters included in C_D also primarily determine K_s inside the canopy, we expect K_s to strongly govern the moisture and heat exchange inside as well as above the taller and forest canopies. The diurnal variation of mean sensible heat flux for the control domain (Fig. 7a) clearly shows the differences between the tall grass canopy and the control run cover in heat transfer above the underlying surface. There are no significant differences before 0800 and after 1800 UTC. The most pronounced differences are around 1200 UTC, reaching a maximum difference of 60 W m^{-2} between the tall grass canopies (50 W m^{-2}) and the control run cover (110 W m^{-2}), whose cover mosaic includes short grass canopies (39.9%), tall grass canopies (4.3%), forest canopies (29.9%), and water and short grass patches (25.9%).

Similar behavior is exhibited by the heat turbulent transfer coefficient between the underlying surface and the lowest model level (Fig. 7b). Its value was derived from the NMM physical package (Janjić 1994, 1996, 2002), using the surface sensible heat flux calculated by LAPS (Mihailovic and Kallos 1997). Because the mosaic of the control run cover is dominated by short grass, the mean heat turbulent transfer coefficient above it during shortwave heating is larger than the coefficient above the control domain that is completely covered by the tall grass canopy (Fig. 7b). This is because the surface temperature T_a of the tall grass canopy is lower than that of the control run cover, as shown in Fig. 8a, resulting in a lower heat exchange coefficient over the tall grass canopy. The instantaneous value of the surface temperature was calculated using Eq. (1). This figure shows that no significant differences occur between the compared cover types during the period between 0000 and 0800 UTC. The minimum of the mean surface temperature for both land use types occurs at approximately the same time, around 0400 UTC. There is not a large difference between the two minima, although the minimum over the tall grass canopy (12.1°C) is slightly higher than that over the control run cover (11.8°C). This difference occurs because the night ground radiation over the tall grass canopy is smaller than that over the control run cover, which consists mostly of short grass and water. The tall grass canopy surface temperature remains higher until 0900 UTC, when the surface temperature of the control run cover becomes higher and stays higher until 0000. The difference between the two maxima is 1.6°C. This difference, resulting from the 3D simulation in which all relevant processes are included, is a clear indication of how greatly the model physics can be affected when the cover in part of the integration domain is changed. Although in this paper we deal specifically with tall grass canopies as an underlying surface, the foregoing analysis is also relevant for assessing the possible impact of various crops on regional climate (Gedney et al. 2000).

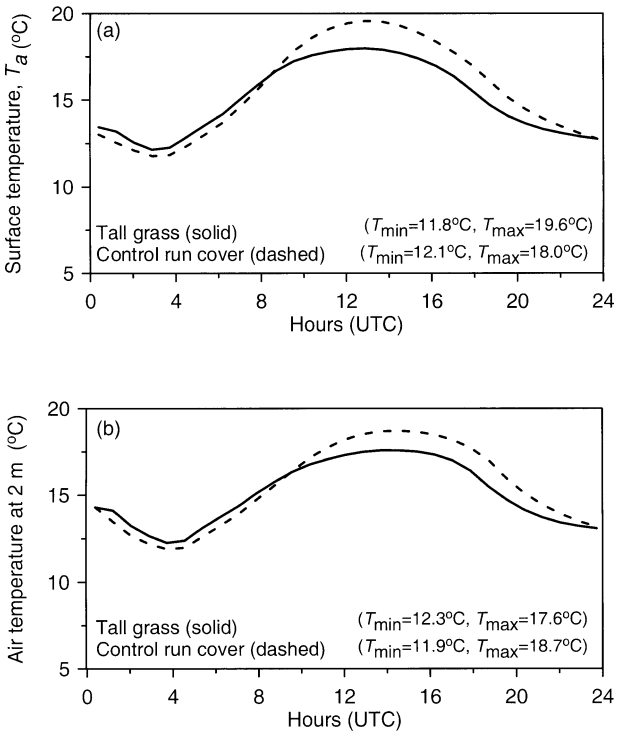

FIG. 8. Temporal variation of the area-averaged (a) surface temperature and (b) air temperature at 2 m for control-run cover and tall grass canopy. The temporal values are obtained by averaging over all grid cells in the control domain.

The air temperature at 2 m is a reliable indicator of the underlying surface's thermal state (i.e., the quality of the surface parameterization), because the surface temperature strongly affects the air temperature at 2 m. This 2-m temperature is determined diagnostically. Figure 8b depicts the temporal variation in this temperature for the control run cover and the tall grass canopy in the control domain. The diurnal behavior of the two curves is close to the behavior of the surface temperature curves in Fig. 8a. However, the 2-m daily amplitudes are smaller than those for the surface temperatures, and the maxima occur later in the afternoon.

Figure 9 depicts the temporal variation of the area-averaged PBL height for the control run cover and tall grass canopy in the control domain. PBL height is one of the most important parameters provided by meteorological models to air-quality models, because it determines the vertical extent of the mixing of air pollutants. PBL height can be affected by many physical processes and parameters, including heat fluxes and ground and near-surface temperatures. This figure shows that the PBL height over the tall grass canopy is lower than that over the control run cover between 1200 and 2000 UTC; the tall grass canopy surface temperature (Fig. 8a) is also lower than the control run surface temperature during this period. This results, for example, in less

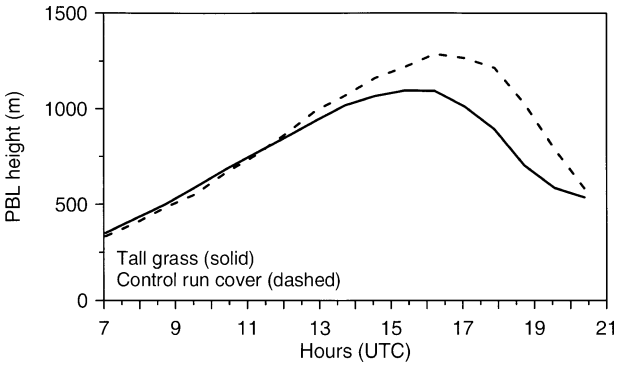

FIG. 9. Temporal variation of the area-averaged PBL height for control-run cover and tall grass canopy. The temporal values are obtained by averaging over all grid cells in the control domain.

rapid vertical mixing of air pollutants over the tall grass area than over the control run area.

To examine how well the proposed expression for K_s and wind speed inside the tall grass canopy represent the influence of the tall grass surface on air temperature, we compared modeled and observed air temperatures at a measurement height of 2 m for 11 stations in areas of mainly tall grass canopy. Figure 10 shows air temperature values obtained from the NMM plotted against observed values taken from the synoptic observations (SYNOP) dataset of 5 June 2002. Figure 10a depicts the comparison for particular times, and Fig. 10b compares the temperature extremes. It can be seen that the model underestimates the 2-m air temperature in the early morning, and the air temperatures simulated for around noon and in the early evening agree well with the observations. For the temperature extremes, the simulated maxima are in better agreement with the observations than are the simulated minima.

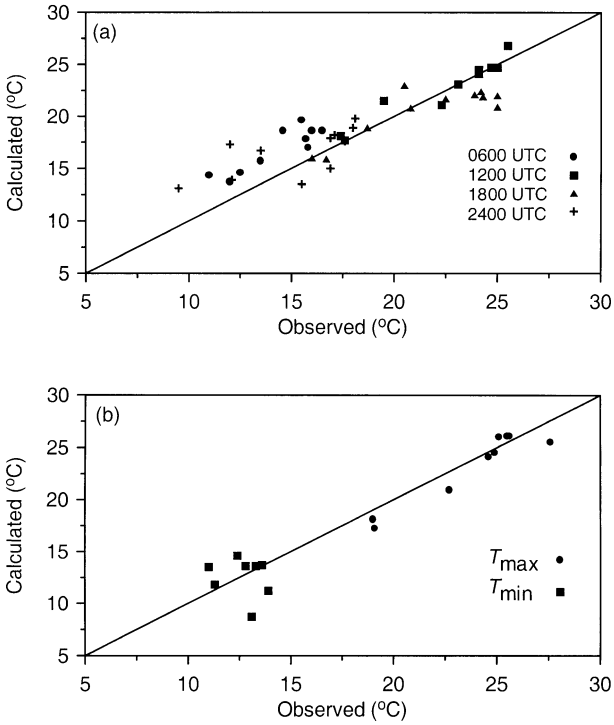

FIG. 10. Air temperatures at 2 m obtained by the NMM (including LAPS) plotted against the observed values taken from the SYNOP data of 5 Jun 2002: (a) comparison for various times, and (b) comparison for the temperatures extremes.

4. Concluding remarks

In this work, we considered and discussed the profiles of turbulent transfer coefficients inside the vegetation canopy and their use for calculating the air temperature inside tall grass canopies in land–atmosphere schemes for environmental modeling. The canopy air space temperature is determined diagnostically from the equality of the canopy's sensible heat flux to some reference level in the atmosphere and the sum of sensible heat flux from the ground and from the leaves to the canopy air volume. Detailed consideration was given to 1) calculations of turbulent fluxes, 2) the shape of the wind and turbulent transfer coefficient profiles, and 3) calculation of the aerodynamic resistances inside tall grass canopies. We focused on tall grass canopies because they can significantly affect the heat and moisture exchange in the lower atmosphere, through key variables like friction velocity and canopy air space temperature. Because the sparseness of a tall grass canopy can affect the wind speed and turbulent transfer coefficients inside the canopy and consequently the internal air temperature, we suggested a method for their calculation. Assuming that the turbulent transfer coefficient inside tall grass is a linear combination of the corresponding coefficients in the space that includes plants and the space above the bare soil fraction, weighted by the fractional cover, we slightly modified the equation that can be solved numerically for the wind profile within the canopy.

To examine how well the proposed calculations of *K*-theory parameters support a simulation of the air temperature inside tall grass canopies, a test was performed using LAPS. Model outputs of canopy air space temperature for 10 days (8–17 July 2002) were compared with single-point micrometeorological measurements over a sunflower field at the Rimski Sancevi experimental site (Serbia). The simulated values agree well with the observations. This agreement results from the suggested parameterization of the scaling length, the canopy source height, the canopy bottom height, and the wind profile beneath the canopy bottom height; the method allows better specification of aerodynamic resistances. However, after midnight the simulated values are lower than the observations, whereas in the early afternoon the simulated values are higher than the observed ones. It is apparent that the calculation of air temperature inside a tall grass canopy strongly depends on the aerodynamic resistances, and, therefore, on their sensitivity to morphological and aerodynamic parame-

ters, which can be sources of uncertainty in their calculation.

To demonstrate how changes in the specification of canopy density affect the simulation of air temperature inside tall grass canopies and, thus, alter the growth of the PBL height, we performed experiments using LAPS coupled with a 1D PBL model over a sunflower canopy. The results showed that an increase in the bare soil fraction leads to increased surface temperature and to rapid growth of the PBL height error. The errors that occur in simulating air temperature inside tall grass canopies and correspondingly in the growth of the PBL height can be ascribed to uncertainties in the calculation of the aerodynamic resistances used in Eq. (1), as is discussed by Sellers and Dorman (1987).

To examine how the turbulent transfer coefficient inside tall grass canopies over a large domain represents the influence of the underlying surface on the air layer above, we designed a numerical experiment involving a 3D simulation using the nonhydrostatic version of the NMM with LAPS implemented in it. The experiment focused on a part of central Europe consisting mostly of agricultural fields, using a dataset from 5 June 2002. The synoptic situation had the following features: The dominant synoptic system over Europe consisted of two cyclonic circulation cells separated by the anticyclone over the Baltic region and a well-developed meridional upper ridge (omega block). A stationary cyclone east of the Carpathian Mountains was filling, and so the surface gradients were weak over eastern Europe and there was no significant baroclinicity at higher levels. The cyclonic field was pronounced at all levels over the western part of the continent. The center of the low with a clear front was over France and moved slowly toward the northeast. There was a strong advection zone over the Alps and the central Mediterranean, while a wide area along the Atlantic seaboard experienced cold-air advection coming from the northwest. The results showed that, within and just above tall grass canopies, buoyancy effects during the daytime are significant. These results could be used to improve the parameterization of turbulent fluxes inside tall grass canopies in land surface schemes, making them more relevant for use in a broad range of practical and scientific activities in environmental and closely related sciences, such as the biophysical parameterization of vegetation in atmospheric, ecological, and agricultural models of all scales.

Last, we compared the air temperature obtained by the NMM against observed values taken from the SYNOP data of 5 June 2002 for 11 stations in areas of mainly tall grass canopy. The model underestimated air temperature at 2 m in the early morning, but around noon and in the early evening model results agreed well with observations. For the temperature extremes, the simulated maxima are in better agreement with the observations than are the simulated minima. To minimize the differences between the simulated and observed air temperatures at 2 m, we plan to improve the parameterization of turbulence within and just above tall grass canopies by conducting additional 3D simulations.

Acknowledgments. This research was supported by the New York State Energy Research and Development Authority under Contractual Agreement NYSERDA 4914-ERTER-ES-99. The research was also supported by the Serbian Ministry for Science and Technology under Contracts BTR.S.02.0401.B and BTR.S.02.0427.B. The investigators thank Dr. S. T. Rao for making valuable comments.

APPENDIX A

The Structure of the Land–Air Parameterization Scheme

The net radiation absorbed by the canopy and soil is assumed to be partitioned into sensible heat, latent heat, and storage terms as

$$R_{\mathrm{nf}} = \lambda E_f + H_f + C_f \frac{\partial T_f}{\partial t} \quad \text{and} \tag{A1}$$

$$R_{\mathrm{ng}} = \lambda E_g + H_g + C_g \frac{\partial T_g}{\partial t}, \tag{A2}$$

where R_{nf} and R_{ng} are net radiation (W m^{-2}), λ is latent heat of vaporization (J kg^{-1}), λE_f and λE_g are evapotranspiration flux (W m^{-2}), H_f and H_g are sensible heat flux (W m^{-2}), C_f and C_g are heat capacity (J K^{-1} m^{-2}), and T_f and T_g are surface temperature (K). The subscripts f and g refer to the upper-level canopy and soil, respectively. The fluxes of sensible and latent heat from the canopy and ground are represented by electrical analog models in which the fluxes are proportional to potential differences (in temperature or vapor pressure) and inversely proportional to resistances, which are equivalent to the inverse integrals of conductances over a specified length scale. For example, an aerodynamic resistance is calculated by integrating the inverse of a turbulent transfer coefficient between the reference points. The LAPS schematic diagram in Fig. A1 (Sellers et al. 1986; Mihailovic and Kallos 1997) shows that these heat fluxes may be written as shown in Eqs. (A3)–(A6):

$$\lambda E_f = \frac{\rho c_p}{\gamma}[e_*(T_f) - e_a]\left(\frac{W_f}{\overline{r_b}} + \frac{1 - W_f}{\overline{r_b} + \overline{r_c}}\right), \tag{A3}$$

where ρ and c_p are the density and specific heat of air (kg m^{-3}, J kg^{-1} K^{-1}), γ is the psychrometric constant (hPa K^{-1}), $e_*(T_f)$ is saturated vapor pressure at temperature T_f (hPa), e_a is canopy air space vapor pressure (hPa), W_f is canopy wetness fraction, $\overline{r_b}$ is bulk canopy boundary layer resistance (s m^{-1}), and $\overline{r_c}$ is bulk canopy stomatal resistance (s m^{-1});

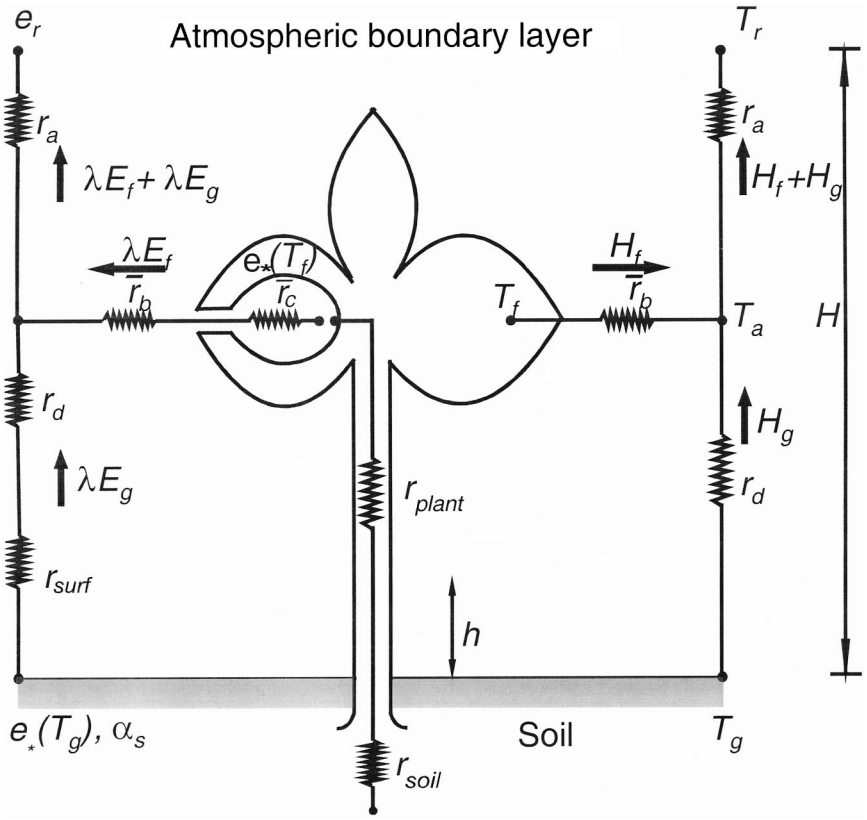

FIG. A1. Schematic diagram of the LAPS. The transfer pathways for latent sensible heat fluxes are shown on the left- and right-hand sides of the diagram, respectively.

$$\lambda E_g = \frac{\rho c_p}{\gamma} \frac{\alpha_s e_*(T_g) - e_a}{r_{\text{surf}} + r_d}, \tag{A4}$$

where α_s is a factor to correct for soil dryness (Mihailovic et al. 1995), $e_*(T_g)$ is saturated vapor pressure at temperature T_g (hPa), r_{surf} is soil surface resistance (s m^{-1}), and r_d is aerodynamic resistance between soil surface and canopy air space (s m^{-1});

$$H_f = \frac{2(T_f - T_a)}{\overline{r_b}} \rho c_p; \quad \text{and} \tag{A5}$$

$$H_g = \frac{(T_g - T_a)}{r_d} \rho c_p, \tag{A6}$$

where T_a is canopy air space temperature (K).

The latent and sensible heat fluxes from the soil and canopy combine to give the total surface fluxes, which are transferred from the canopy air space to the reference height z_r and are given by

$$\lambda E_f + \lambda E_g = \frac{(e_a - e_r)}{r_a} \frac{\rho c_p}{\gamma} \quad \text{and} \tag{A7}$$

$$H_f + H_g = \frac{(T_a - T_r)}{r_a} \rho c_p, \tag{A8}$$

where e_r is vapor pressure at the reference height (hPa), r_a is aerodynamic resistance (s m^{-1}), and T_r is air temperature at the reference height (K).

Substituting (A3)–(A8) into (A1) and (A2) yields two differential equations for T_f and T_g. These are solved simultaneously using a backward implicit method.

APPENDIX B

Derivation of the Equation for Wind Profile inside a Canopy in the Sandwich Approach

Let us consider an element of the canopy volume having an area S and height H. The loss of air particles' momentum because of close contact with the plant leaves comes from the drag force arising on the leaf surface. This drag force F_d produces a shearing such that $d\tau/dz$, the vertical gradient of shear stress τ is equal to the drag force per volume V; that is,

$$d\tau/dz = F_d/V. \tag{B1}$$

The drag force per leaf unit area S_l is parameterized to be proportional to the wind speed, u, that is, the volumetric kinetic energy $1/2\rho u^2$ with the coefficient of proportionality C_d, the leaf drag coefficient. So,

$$\frac{F_d}{S_l} = \frac{1}{2} C_d \rho u^2, \tag{B2}$$

where ρ is the air density. Note that S_l is the area of all leaves in the considered volume. Following the definition of leaf area index (LAI), we can write LAI = $(1/2)(S_l/S)$, because LAI is defined in terms of only one side of the leaf. Using $\tau = \rho K_s(du/dz)$ (where K_s is the turbulent transfer coefficient) and Eqs. (B1) and (B2) and keeping in mind that the volume occupied by plants is *SH*, after some manipulation we arrive at

$$\frac{d}{dz}\left(K_s\frac{du}{dz}\right) = \frac{C_d\overline{L_d}(H - h)}{H}u^2, \qquad \text{(B3)}$$

where $\overline{L_d}$ is the area-averaged canopy density and h is the canopy bottom height.

REFERENCES

Alapaty, K., J. E. Pleim, S. Raman, D. S. Niyogi, and D. W. Byun, 1997a: Simulation of atmospheric boundary layer processes using local- and nonlocal-closure schemes. *J. Appl. Meteor.,* **36,** 214–233.

——, S. Raman, and D. S. Niyogi, 1997b: Uncertainty in the specification of surface characteristics: A study of prediction errors in the boundary layer. *Bound.-Layer Meteor.,* **82,** 473–475.

Ayers, F., Jr., 1952: *Theory and Problems of Differential Equations.* Shaum, 296 pp.

Blackadar, A. K., 1976: Modeling the nocturnal boundary layer. Preprints, *Third Symp. on Atmospheric Turbulence Diffusion and Air Quality,* Raleigh, NC, Amer. Meteor. Soc., 46–49.

——, 1978: Modeling pollutant transfer during daytime convection. Preprints, *Fourth Symp. on Atmospheric Turbulence Diffusion and Air Quality,* Reno, NV, Amer. Meteor. Soc., 443–447.

Brandmeyer, J., and H. A. Karimi, 2001: Coupling methodologies for environmental models. *Environ. Modell. Software,* **15,** 479–488.

Brunet, Y., J. J. Finnigan, and M. R. Raupach, 1994: A wind tunnel study of air flow in waving wheat: Single-point velocity statistics. *Bound.-Layer Meteor.,* **70,** 95–132.

Brutsaert, W., and M. Sugita, 1996: Sensible heat transfer parameterization for surfaces with anisothermal dense vegetation. *J. Atmos. Sci.,* **53,** 209–216.

Denmead, O. T., 1976: Temperate cereals. *Vegetation and the Atmosphere,* 2d ed., J. L. Monteith, Ed., Academic Press, 1–31.

Dickinson, R. E., A. Henderson-Sellers, P. Kennedy, and M. Wilson, 1986: Biosphere Atmosphere Transfer Scheme (BATS) for the NCAR Community Climate Model. NCAR Tech. Note NCAR/TN275+STR, 69 pp.

Dubov, A. S., L. P. Bikova, and S. V. Marunich, 1978: *Turbulence Inside a Canopy* (in Russian). Gidrometeoizdat, 184 pp.

Estoque, M. A., 1968: Vertical mixing due to penetrative convection. *J. Atmos. Sci.,* **25,** 1046–1051.

Gedney, N., P. M. Cox, H. Douville, J. Polcher, and P. J. Valdes, 2000: Characterizing GCM land surface schemes to understand their responses to climate change. *J. Climate,* **13,** 3066–3079.

Goudriaan, I., 1977: *Crop Micrometeorology: A Simulation Study.* Wageningen Center for Agricultural Publishing and Documentation, 211 pp.

Henderson-Sellers, A., 1996: Soil moisture simulation: Achievements of the RICE and PILPS intercomparison workshop and future directions. *Global Planet. Change,* **13,** 99–115.

Janjié, Z. I., 1994: The step mountain eta coordinate model: Further developments of the convection, viscous sublayer, and turbulence closure schemes. *Mon. Wea. Rev.,* **122,** 927–945.

——, 1996: The surface layer in the NCEP Eta Model. Preprints, *11th Conf. on Numerical Weather Prediction,* Norfolk, VA, Amer. Meteor. Soc., 354–355.

——, 2002: Nonsingular implementation of the Mellor–Yamada 2.5 scheme in the NCEP Meso Model. NCEP Office Note No. 437, 61 pp.

——, J. P. Gerrity Jr., and S. Nickovic, 2001: An alternative approach to nonhydrostatic modeling. *Mon. Wea. Rev.,* **129,** 1164–1178.

Katul, G. G., and W.-H. Chang, 1999: Principal length scales in second-order closure models for canopy turbulence. *J. Appl. Meteor.,* **38,** 1631–1643.

Lalic, B., D. T. Mihailovic, B. Rajkovic, I. D. Arsenic, and D. Radlovic, 2003: Wind profile within the forest canopy and in the transition layer above it. *Environ. Modell. Software,* **18,** 947–950.

Laval, K., 1988: Land surface processes. *Physically Based Modelling and Simulation of Climate and Climatic Change—Part 1,* M. E. Schlesinger, Ed., Kluwer Academic, 285–306.

Legg, B. J., and I. F. Long, 1975: Turbulent diffusion within a wheat canopy II. *Quart. J. Roy. Meteor. Soc.,* **101,** 611–628.

Massman, W. J., and J. C. Weil, 1999: An analytical one-dimensional second-order closure model of turbulence statistics and the Lagrangian time scale within and above plant canopies of arbitrary structure. *Bound.-Layer Meteor.,* **91,** 81–107.

Mihailovic, D. T., 1996: Description of a land–air parameterization scheme (LAPS). *Global Planet. Change,* **13,** 207–215.

——, 2003: Implementation of Land–Air Parameterization Scheme (LAPS) in a limited area model. The New York State Energy Conservation and Development Authority Final Rep. 4914-ERTER-ER-99, 110 pp.

——, and B. Rajkovic, 1993: Surface vegetation parameterization in atmospheric models: A numerical study. *Meteor. Z.,* **2,** 239–243.

——, and G. Kallos, 1997: A sensitivity study of a coupled soil–vegetation boundary layer scheme for use in atmospheric modeling. *Bound.-Layer Meteor.,* **82,** 283–315.

——, R. A. Pielke, B. Rajkovic, T. J. Lee, and M. Jeftic, 1993: A resistance representation of schemes for evaporation from bare and partly plant-covered surfaces for use in atmospheric models. *J. Appl. Meteor.,* **32,** 1038–1054.

——, B. Rajkovic, B. Lalic, and L. J. Dekic, 1995: Schemes for parameterizing evaporation from a non-plant-covered surface and their impact on partitioning the surface energy in land–air exchange parameterization. *J. Appl. Meteor.,* **34,** 2462–2475.

——, T. J. Lee, R. A. Pielke, B. Lalic, I. Arsenic, B. Rajkovic, and P. L. Vidale, 2000: Comparison of different boundary layer schemes using single point micrometeorological field data. *Theor. Appl. Climatol.,* **67,** 135–151.

——, I. Koci, B. Lalic, I. Arsenic, D. Radlovic, and J. Balaz, 2001: The main features of BAHUS-biometeorological system for messages on the occurrence of diseases in fruits and vines. *Environ. Modell. Software,* **16,** 691–696.

——, S. T. Rao, C. Hogrefe, and R. Clark, 2002: An approach for the aggregation of aerodynamic parameters in calculating the turbulent fluxes over heterogeneous surfaces in atmospheric models. *Environ. Fluid Mech.,* **2,** 315–337.

Munley, W. G., 1991: Estimation of regional evapotranspiration for tall grass prairie measurements of properties of the atmospheric boundary layer. *Water Resour. Res.,* **27,** 225–230.

Pielke, R. A., Sr., 2002a: *Mesoscale Meteorological Modeling.* 2d ed. Academic Press, 676 pp.

——, 2002b: Overlooked issues in the U.S. national climate and IPCC assessments. An editorial essay. *Climatic Change,* **52,** 1–11.

Pinard, J. D. J.-P., and J. D. Wilson, 2001: First- and second-order models for wind in a plant canopy. *J. Appl. Meteor.,* **40,** 1762–1768.

Raupach, M. R., J. J. Finnigan, and Y. Brunet, 1996: Coherent eddies and turbulence in vegetation canopies: The mixing-layer analogy. *Bound.-Layer Meteor.,* **78,** 351–382.

Richtmyer, R. D., and K. W. Morton, 1967: *Difference Methods for Initial Value Problems.* Interscience, 406 pp.

Rodhe, H., H. Charlson, and T. L. Anderson, 2000: Avoiding circular logic in climatic modeling. An editorial essay. *Climatic Change,* **44,** 409–411.

Sellers, P. J., and J. L. Dorman, 1987: Testing the Simple Biosphere

model (SiB) using point micrometeorological and biophysical data. *J. Climate Appl. Meteor.,* **26,** 622–651.

——, Y. Mintz, Y. Sud, and A. Dalcher, 1986: A Simple Biosphere model (SiB) for use within general circulation model. *J. Atmos. Sci.,* **43,** 506–531.

——, W. J. Shuttleworth, J. L. Dorman, A. Dalcher, and J. M. Roberts, 1989: Calibrating the Simple Biosphere model for Amazonian tropical forest using field and remote sensing data: Part 1. Average calibration with field data. *J. Appl. Meteor.,* **28,** 727–759.

Staub, B., and C. Rosenzweig, 1987: Global digital datasets of soil type, soil texture, surface slope, and other properties: Documentation of archived tape data. NASA Tech. Memo. 100685, 19 pp.

Uchijima, Z., 1976: Radiation characteristics of maize and rice fields. *Vegetation and the Atmosphere,* 2d ed., J. L. Monteith, Ed., Academic Press, 32–45.

van den Hurk, B. J. J. M., 1996: Sparse canopy parameterizations for meteorological models. Ph.D. dissertation, Wageningen Agricultural University, 271 pp.

van Pul, W. A. J., 1992: The flux of ozone to a maize crop and underlying soil during a growing season. Ph.D. dissertation, Wageningen Agricultural University, 147 pp.

Walko, R. L., and Coauthors, 2000: Coupled atmosphere–biophysics–hydrology models for environmental modeling. *J. Appl. Meteor.,* **39,** 931–944.

Wilson, J. D., D. P. Ward, G. W. Thurtell, and G. E. Kidd, 1982: Statistics of atmospheric turbulence within and above a corn canopy. *Bound.-Layer Meteor.,* **24,** 495–519.

Wyngaard, J. C., 1988: Convective processes in the lower atmosphere. *Flow and Transport in the Natural Environment: Advances and Applications,* W. L. Steffen and O. T. Denmead, Eds., Springer, 240–260.

Xue, Y. K., P. J. Sellers, J. K. Kinter, and J. Shukla, 1991: A simplified biosphere model for global climate studies. *J. Climate,* **4,** 345–364.

Zhang, D., and R. A. Anthes, 1982: A high-resolution model of the planetary boundary layer—Sensitivity tests and comparisons with SESAME-79 data. *J. Appl. Meteor.,* **21,** 1594–1609.

Zoumakis, N. M., 1993: Estimating the zero-plane displacement and roughness length for tall vegetation and forest canopies using semi-empirical wind profiles. *J. Appl. Meteor.,* **32,** 574–579.